A celestial reference frame based on Kalman filtering

B. Soja, R. Gross, C. Jacobs, T. Chin, C. Abbondanza, M. Heflin, J. Parker, X. Wu, M. Karbon, T. Nilsson, R. Heinkelmann, H. Schuh

Abstract In this study, we investigate a novel approach to the determination of celestial reference frames (CRF). Instead of a constant model for radio sources positions, we adopt a time series representation, which allows temporal variations of radio source coordinates to be taken into account. In particular, the added flexibility is beneficial for radio sources with extended structure. We compute our time series-based CRF solutions by Kalman filtering and smoothing radio source positions, which are initially obtained from single-session VLBI analysis. The temporal resolution of the estimated CRF coordinates is identical to that of the input data, i.e. usually 1-4 days. The magnitude of the coordinate variations is controlled by the amount of process noise applied in the filter, which is in turn derived from analyzing the Allan standard deviation of the corresponding radio source coordinate time series. Measures have been developed to reduce the impact of observation errors and datum effects on the noise model.

Keywords Kalman filter, celestial reference frame, source structure

Benedikt Soja, Richard S. Gross, Christopher S. Jacobs, Toshio M. Chin, Michael B. Heflin, Jay W. Parker, Xiaoping Wu
Jet Propulsion Laboratory, California Institute of Technology, 4800 Oak Grove Dr, Pasadena, CA 91109, United States of America
Maria Karbon, Tobias Nilsson, Robert Heinkelmann, Harald Schuh
GFZ German Research Centre for Geosciences, Telegrafenberg, D-14473 Potsdam, Germany
Harald Schuh
Technische Universität Berlin, Straße des 17. Juni 135, D-10623 Berlin, Germany

1 Introduction

Extragalactic radio sources exhibit time variability, for example, due to source structure and changes therein as well as hour angle and frequency variability. In the analysis of VLBI data and in the determination of celestial reference frames (CRFs), source structure effects are commonly not corrected (IERS Conventions, 2010), which may lead to a degradation of the quality of the VLBI products and frames. Currently, no source structure correction models exist that could be utilized by analysis centers with little effort. Likewise, the International Celestial Reference Frame 2 (ICRF2, Fey et al, 2015) is based on a constant coordinate model for radio sources, neglecting any temporal variability. A group of radio sources characterized as ”special handling sources” has been reduced during the estimation of the ICRF2, however, the published catalog, used in the VLBI analysis, only includes constant coordinates.

An approach for considering the time variability of radio sources is to extend the coordinate model of radio sources. Karbon et al (2016) used linear splines instead of a constant coordinate model to create a CRF, which allowed strong but unstable sources to be included in the datum when applied in VLBI analysis. Especially the insufficient observation geometries in the early years of VLBI benefited from the increased selection of datum sources and the estimated nutation parameters were improved by 10%.

In this work, we take a different approach to consider radio source coordinate variabilities: a time series representation. The tool of choice is Kalman filtering, which sequentially assimilates the observational data to estimate source coordinates with high temporal resolution. The source positions are assumed to be stochastic processes, reflecting the physical nature of these objects. A potential disadvantage of the Kalman filter algorithm is a higher computational demand compared to a classical least-squares inversion.

Kalman filtering already has been successfully used in the creation of terrestrial reference frames (Wu et al, 2015; Soja et al, 2016). In the future, the International Earth Rotation and Reference Systems Service (IERS) International Terrestrial Reference System (ITRS) Combination Center at Jet Propulsion Laboratory (JPL) aims to jointly determine terrestrial and celestial reference frames, and Earth orientation parameter (EOP) time series in order to eliminate current inconsistencies. In order to achieve a joint determination, the estimation of the CRF has to be integrated into the filter-based software KALREF, which has, for example, been used to determine the JTRF2014, the recent ITRF solution by JPL (Abbondanza et al, 2017).

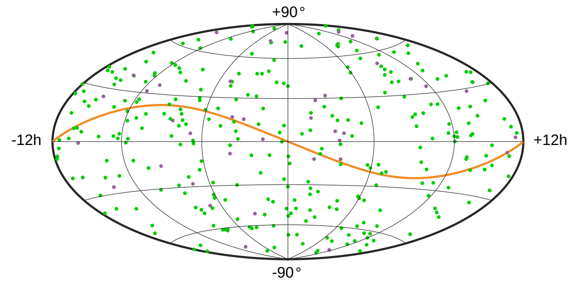

Fig. 1 Sky map of the radio sources included in this study, with dots representing defining sources, purple dots special handling sources, and the orange line the ecliptic.

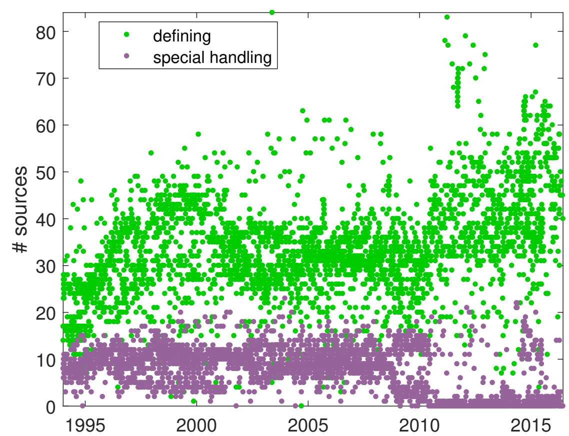

Fig. 2 The number of defining (green) and special handling (purple) radio sources per VLBI session is plotted against time.

2 Data and Methodology

2.1 VLBI data

Only a limited data set was selected for the preliminary tests and investigations presented in this work. 3118 IVS VLBI sessions were chosen covering the time period between 1994 and 2016.5. In total, 334 radio sources were considered in this study, with 295 defining sources and 39 special handling as categorized in the ICRF2. Figure 1 shows the radio source distribution in the sky, with the majority (189 out of 334) being located in the Northern celestial hemisphere. The number of radio sources observed per session, distributed among the two categories, is displayed in Fig. 2. From around 2010 onward, the number of observed special handling sources has been drastically reduced in favor of defining sources. Hence, an improved treatment of the special handling sources, which are typically subject to source structure, is expected to have the largest impact in the early years.

2.2 VLBI analysis

The individual VLBI sessions were processed using the least-squares module of the VieVS@GFZ software (Nilsson et al, 2015). Correction models were applied according to IERS Conventions (2010) and the estimated parameters include radio sources (No-Net-Rotation constraints w.r.t. ICRF2 defining sources), all five EOP, station coordinates (No-Net-Translation and -Rotation constraints w.r.t. ITRF2014) and auxiliary parameters for clocks and troposphere. Only radio sources with three or more observations were estimated, the rest are constrained to their a priori positions.

2.3 Kalman filter setup

The estimated radio source coordinates and their covariances from the single session analysis serve as input to the Kalman filter for CRF determination. The Kalman filter is run both forward and backward in time, followed by a smoothing operation to average the estimated state vectors from the two runs. The state vector, containing the radio source coordinates, is updated for every single VLBI session (usually every 1-4 days). The coordinates are assumed to behave like random walk processes, which are easy to implement in a Kalman filter and have already been successfully applied in the creation of terrestrial reference frames (Soja et al, 2016). A source-based process noise model is utilized as described in Section 3. The datum is preserved from the single session solutions. The output consists of the filtered and smoothed radio source coordinate time series (i.e., right ascension α and declination δ).

3 Process noise of radio source coordinates

In the Kalman filter, the process noise regulates how much weight is given to the observations in relation to the predictions based on the functional model. In general, it is desirable to utilize external information to create the process noise model, which in the case of radio sources proves to be difficult. Observations at different radio or optical frequencies might not translate to the behavior of sources at geodetic VLBI's S- and X-bands. Radio source images and structure indices could be useful, but it is not clear how they can be converted to values of process noise. Additionally, the effect of outlier flagging during both the correlation and analysis processes is likely to alter the impact of source structure on the estimated coordinates.

For these reasons, it was decided to use the same time series of radio source positions to derive the noise model that are used to determine the CRF. As described in Soja et al (2015), the Allan standard deviation (ADEV) served as the tool of choice to determine the stochastic behavior of the 334 radio sources. Fig. 3 shows the ADEV for each individual radio source's right ascension time series and the average ADEV over all sources. Fitting a power-law model to the ADEV, the exponent k is almost identical to -1, indicating a perfect white noise process. Even for a radio source with extensive source structure like 4C 39.25 (Fig. 4), the same holds true. It is thus suspected that observational errors and datum effects are primarily the cause for the whiteness of the noise. The magnitude of the

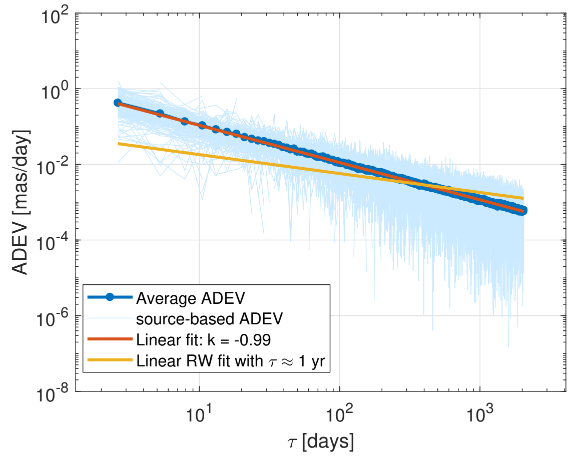

Fig. 3 ADEV for the right ascension ($\alpha \cos\delta$) time series of the individual radio sources (light blue) and the averaged ADEV of all sources (dark blue). A power-law fit is shown in red, and one assuming a random walk process in yellow.

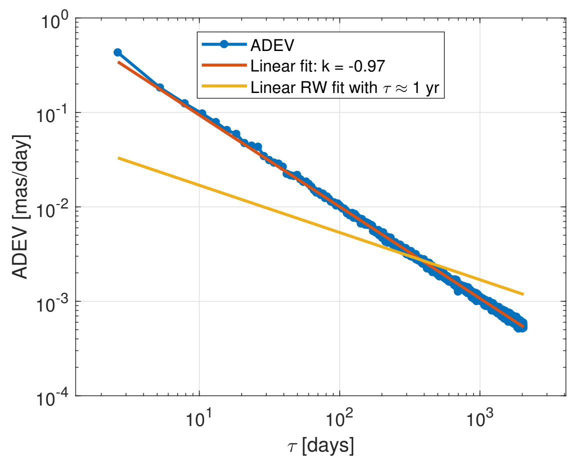

Fig. 4 ADEV and power-law fits to it (like in Fig. 3) are shown for the radio source 4C 39.25.

white noise seems to dominate contributions due to other reasons, such as source structure.

To remove some of the random observation error and datum effects, half-yearly averages of the positions were used instead of single-session coordinates. At least 20 data points were required per interval, which was fulfilled by 66 of the sources. The ADEV based on the half-yearly averages, shown in Fig. 5, indicates that on average, the stochastic process is no longer perfect white noise. In fact, some of the radio sources, such as 4C 39.25 (Fig. 6), exhibit temporal correlation and are better characterized by a random walk than by a white noise process.

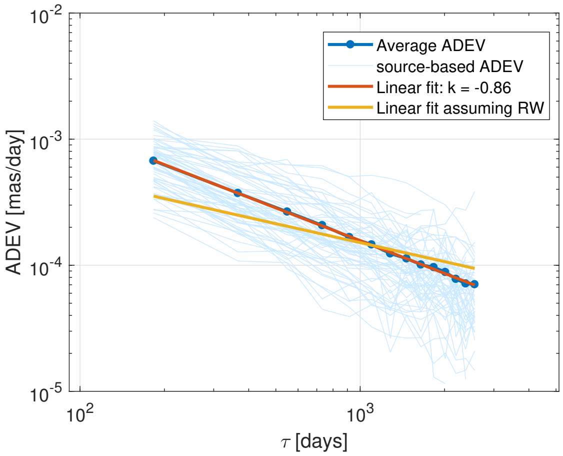

Fig. 5 Like Fig. 3, but for time series of half-yearly averages.

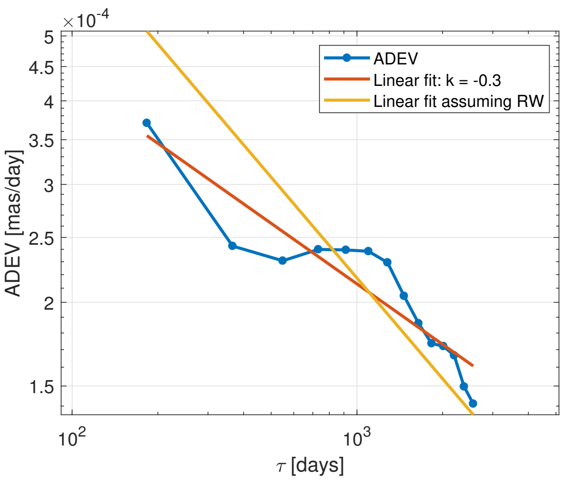

Fig. 6 Like Fig. 4, but for a time series of half-yearly averages.

The power spectral densities (PSDs) of the white noise driving the random walk processes are individually estimated for the 66 radio sources as outlined in Soja et al (2015). Sky maps of the source-based process noise are shown in Fig. 7. The average PSD over all sources of $\alpha \cos \delta$ is 28 µas^2/day, and for declination it is 72 µas^2/day. The declination process noise being more than twice as large is likely related to the worse VLBI network geometry in North-South direction. Another indication that the declination process noise is more strongly affected by artificial errors is that the radio sources at about -30° tend to have larger PSD values. Since most radio telescopes are in the Northern hemisphere, these sources are more often observed at low elevation angles, increasing tropospheric errors.

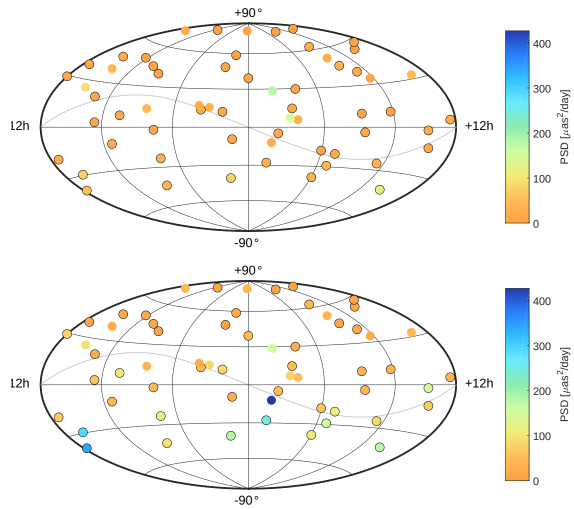

Fig. 7 Color-coded PSD values for 66 sources based on half-yearly averaged time series. Black circles indicate defining sources. Top: $\alpha \cos \delta$, bottom: δ.

Missing cable calibration at some of the Southern telescopes might contribute to this effect as well. In right ascension, the average PSD values of special handling sources are about two times as large as those of the defining sources (21 vs. 50 µas^2/day), while the difference is much smaller in the case of declination (69 vs. 83 µas^2/day). The only explanation for the different ratios is once again a stronger contribution of artificial errors to δ compared to α.

4 Kalman filter CRF solutions

Three CRF solutions have been computed using the Kalman filter as described in the previous sections, with the noise model as the only difference. In the first solution, the process noise was set to zero, resulting in a deterministic solution with constant radio source positions. Next, the source-based process noise model derived from the single-session coordinates was applied. Finally, the source-based noise model from the half-yearly averages was used for 66 sources (cf. Fig. 7), and the rest was estimated deterministically.

The different solutions are shown for radio source 4C 39.25 in Fig. 8. The deterministic estimate differs from ICRF2 by about 100 µas, most likely stemming from the different data time spans. The solution with the noise model from the individual VLBI ses-

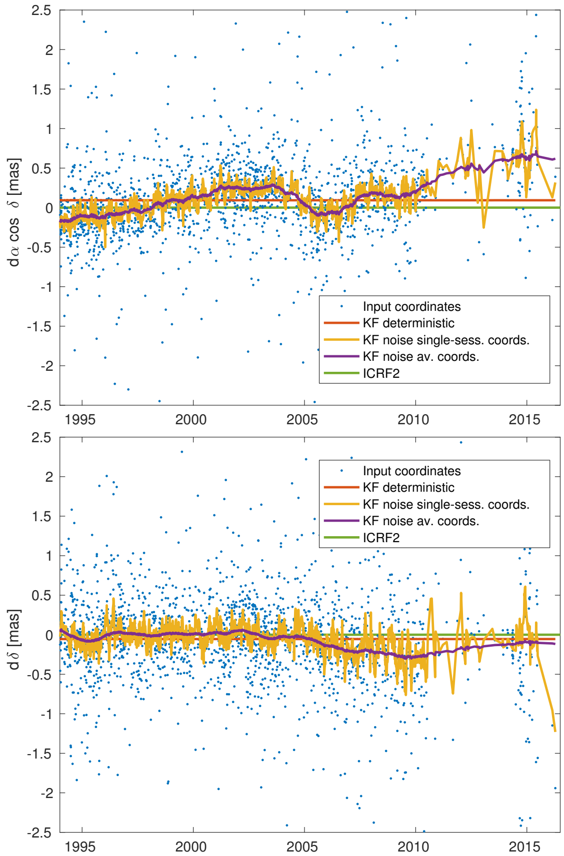

Fig. 8 Time series of radio source coordinates w.r.t. ICRF2 (top: right ascension, bottom: declination) of 4C 39.25 based on the Kalman filter CRF solutions described in Section 4.

sions exhibits large scatter, which seems to be related to the artificial error sources discussed above. The CRF based on the half-yearly averages smoothly follows what seems to be a signal caused by changes in the structure of the source. In right ascension, a long-term sawtooth pattern can be recognized, typically caused by a component of the source structure emerging from the core and first moving out of the narrow X-band beam and later out of the wide S-band beam over several years. In declination, the CRF time series is much less variable. Images of this radio source (e.g., from vlbi.obs.u-bordeaux1.fr) show that the source is a two-component source when observed in X-band with the two components in equatorial direction, explaining the signal seen in the CRF solution.

5 Conclusions

This study includes preliminary results related to a first demonstration of a Kalman filter CRF. The time series approach allows to take into account temporal variability in radio source positions. A source-based noise model was derived from statistical analysis of the radio source time series using ADEV. By computing the noise model from half-yearly-averaged radio source positions, the scatter in the CRF time series was reduced. In a case study of radio source 4C 39.25, the Kalman filter was able to track a signal in the source coordinates typical of a two-component radio source.

In the future, the input data will be extended, in particular, the number of radio sources. Other approaches for determining the noise model will be explored, for example, by considering the structure index or the direction of the jet. Finally, strategies for the evaluation of Kalman filter CRFs and the underlying process noise models will be developed and executed.

Acknowledgements: The authors thank the IVS for providing the VLBI data used in this work (Nothnagel et al, 2015). B. Soja's research was supported by an appointment to the NASA Postdoctoral Program at Jet Propulsion Laboratory, administered by USRA under contract with NASA.

References

Abbondanza et al (2017) JTRF2014, the JPL Kalman Filter and Smoother Realization of the ITRS. JGR, submitted.

Fey et al (2015) The 2nd Realization of the ICRF by VLBI. AJ 150(2):58

IERS Conventions (2010) G. Petit and B. Luzum (eds.). IERS Technical Note 36, Frankfurt am Main: Verlag des BKG

Karbon et al (2016) The extension of the parametrization of the radio source coordinates in geodetic VLBI. JoG, DOI 10.1007/s00190-016-0954-1

Nilsson et al (2015) Application of Kalman filtering in VLBI data analysis. EPS 67(1):136, DOI 10.1186/s40623-015-0307-y

Nothnagel et al (2015) The IVS data input to ITRF2014. GFZ Data Services, DOI 10.5880/GFZ.1.1.2015.002

Soja et al (2015) Tropospheric delay determination by Kalman filtering VLBI data. EPS 67(1):144, DOI 10.1186/s40623-015-0293-0

Soja et al (2016) Determination of a TRF via Kalman filtering of VLBI data. JoG, DOI 10.1007/s00190-016-0924-7

Wu et al (2015) KALREF – A Kalman filter and time series approach to the ITRF realization. JGR: Solid Earth, pp 3775–3802, DOI 10.1002/2014JB011622